ISSN 1070-4272, Russian Journal of Applied Chemistry, 2015, Vol. 88, No. 10, pp. 1576−1581. © Pleiades Publishing, Ltd., 2015.
Original Russian Text © E.A. Mezina, I.M. Lipatova, 2015, published in Zhurnal Prikladnoi Khimii, 2015, Vol. 88, No. 10, pp. 1390−1395.

VARIOUS PHYSICOCHEMICAL AND TECHNOLOGICAL PROCESSES

Effect of Peroxide Depolymerization of Chitosan on Properties of Chitosan Sulfate Particles Produced from This Substance

E. A. Mezina and I. M. Lipatova

Krestov Institute of Solution Chemistry, Russian Academy of Sciences, ul. Akademicheskaya 1, Ivanovo, 153045 Russia
e-mail: aay@isc-ras.ru

Received May 28, 2015

Abstract—Effect of the oxidative destruction of chitosan on the rate at which a dispersed phase is formed in its dilute solutions in the presence of sulfate ions and on the composition, size and ζ-potential of submicrometer chitosan sulfate particles being formed was studied. It was found that the particle size steadily decreases as the molecular mass of chitosan becomes smaller, and the sedimentation stability of aqueous dispersions increases in the absence of surfactants. The $\nu_{SO_4} : \nu_{NH_2}$ molar ratio in chitosan sulfate particles is independent of the molecular mass of chitosan and varies within the range 0.45–0.46. A pH-dependence of the sign of the ζ-potential with isoelectric point at pH 5.0 was found for particles based on destructed chitosan.

DOI: 10.1134/S1070427215100031

Chitosan is a polyglucosamine of natural origin, produced by alkaline deacetylation of chitin. Owing to a set of unique properties (biocompatibility, mucoadhesiveness, biodegradability, low toxicity, etc.), this polymer finds steadily increasing use in various fields of medicine and pharmacology. Of considerable interest are aqueous dispersions formed by meso- and nanosize particles of chitosan, which can be used as carriers for medicinal substances [1–3]. One of simple ways to obtain dispersions of this kind is via precipitation due to the electrostatic interaction of protonated amino groups of chitosan with polycharged anions and, in particular, with tripolyphosphate and sulfate [3–5]. When meso- and nanosize particles are obtained on the basis of chitosan, it is subjected to a preliminary depolymerization. This is done by acid hydrolysis [6], enzymatic depolymerization [7], and oxidative destruction with persulfates [5] or sodium nitrite [4]. Te well-known method for depolymerization of chitosan uses hydrogen peroxide [8, 9]. The advantage of this method is in its accessibility, ecological safety, no need to purify the product to remove destructing agents, and minimization of side reaction of oxidation of functional groups under the mild conditions of the process [9]. The method and conditions of a preliminary destruction of chitosan largely affect the characteristics of submicrometer particles obtained on its basis. The most important characteristics essentially determining the transport properties of carrier particles are their size and electrokinetic potential.

The goal of our study was to examine the influence exerted by the conditions of preliminary destruction of chitosan by hydrogen peroxide on the composition, size, and ζ-potential of chitosan particles produced by the ion precipitation method.

EXPERIMENTAL

We used commercial chitosan of domestic manufacture (Bioprogress, Shchelkovo) with a molecular mass (MM) of 1.95 105 and degree of deacetylation (DDA) of 0.82.

The DDA of chitosan was determined by potentiometric titration [10].

Starting chitosan solutions were prepared by dispersion of weighed portions of the polymer in water, followed by addition of acetic acid in amount of 2 wt %. The dissolution was performed under permanent agitation for 2 h, after which the solutions were allowed to stay for 20 h more.

To obtain chitosan derivatives with lowered degree of polymerization, the destruction of chitosan with hydrogen

peroxide was performed under homogeneous conditions. The process was performed at 50°C with a 0.6% chitosan solution in 2% acetic acid. The concentration of H_2O_2 was 0.8 wt %. A set of chitosan samples with various MM was obtained by varying the reaction duration within the range 30–120 min.

IR spectra of the starting and depolymerized chitosan samples were recorded with a VERTEX 80v IR spectrometer (Germany) in the range 2000–500 cm^{-1}. To measure the spectra, chitosan samples were pelletized with KBr in a 1 : 100 ratio.

The MM of chitosan samples was determined by viscometry by using the Mark–Kuhn–Houwink equation: $[\eta] = KM^{\alpha}$. For chitosan in an acetate buffer solution, $K = 1.464 \times 10^{-4}$ and $\alpha = 0.885$. The characteristic viscosity of chitosan was determined by the extrapolation method at 25°C on an Ubbelohde viscometer (capillary diameter 0.56 mm) in 2% acetic acid. Sodium acetate (0.2 M) was introduced as a supporting electrolyte; the pH of the resulting buffer solution was 5.4.

Dispersions of chitosan sulfate particles were prepared by the procedure described in [12].

Kinetic curves describing the variation of the state of mixed solutions of chitosan and a salt were obtained by sampling these mixtures continuously agitated on a magnetic rabble and measuring their optical density. The optical densities were measured with an SF-58 spectrophotometer (LOMO, Russia) at a wavelength $\lambda = 500$ nm in standard glass cuvettes with optical path length of 1 cm.

The particle size was determined by the dynamic light-scattering method, and the ζ-potential, by the method of electrophoretic light scattering on a Zetasizer Nano, Malvern Zetasize analyzer of the particle size and ζ-potential (Malvern Instruments Ltd., Great Britain).

The elemental composition of chitosan sulfate particles was determined with a Flash HCNS-0 EA 1112 chromatographic analyzer (Termo Quest, Italy).

RESULTS AND DISCUSSION

Figure 1 shows the kinetic curve describing how the MM of chitosan decreases in the course of its oxidative destruction by hydrogen peroxide under homogeneous conditions at a temperature of 50°C. It would be expected under the chosen conditions (0.6% chitosan, 2% CH_3COOH, and 0.8% H_2O_2) that acid hydrolysis should make a certain contribution to the destruction.

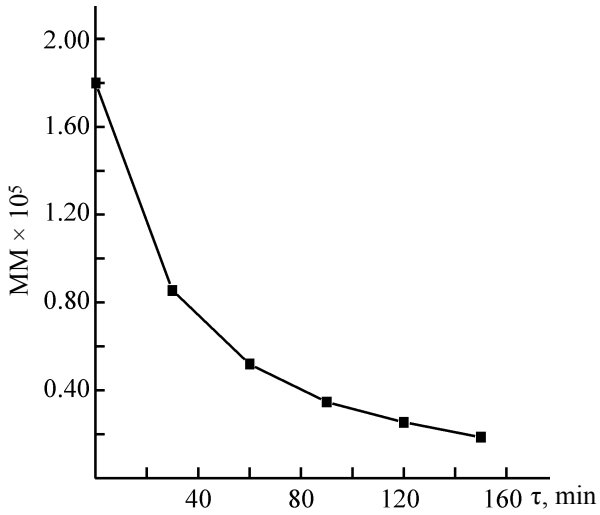

Fig. 1. Kinetic curve describing the destruction of chitosan by hydrogen peroxide under homogeneous conditions. (MM) Molecular mass and (τ) time. $T = 50$°C, $c_{H_2O_2} = 0.8\%$, $c_{chitosan} = 0.6\%$, $c_{CH_3COOH} = 2\%$.

The authors of [9] demonstrated experimentally that the contribution of the acid hydrolysis is insignificant even at the substantially lower H_2O_2 concentration at the same relative amounts of chitosan and CH_3COOH. It is known that the destruction of chitosan under the action of hydrogen peroxide is due to the rupture of glycoside bonds by the free-radical mechanism [13, 14]. According to published data [9, 14, 15], the contribution of oxidative processes yielding new oxygen-containing groups is determined in the peroxide destruction of chitosan by the process conditions, primarily by the concentration of the peroxide and temperature. A conclusion was made in [9] that mostly C–O–C bonds are ruptured under mild conditions ($T < 50$°C, $c_{H_2O_2} < 2\%$) there occurs no opening of the pyranose ring and deamination. It was noted in other reports that OH groups of chitosan can be oxidized to give oxygen-containing, including carboxy, groups [14, 15].

To assess the possible chemical changes caused in chitosan by its treatment with hydrogen peroxide under the experimental conditions of the present study, we measured IR spectra of the starting chitosan and depolymerizates (Fig. 2). Preliminarily, the samples were precipitated from acetic acid solutions with sodium hydroxide, washed, and dissolved in hydrochloric acid. Samples for recording of IR spectra were produced from hydrochloric acid solutions by drying. These measures are necessary for removing acetic acid and converting the supposed COO^- groups to undissociated COOH groups

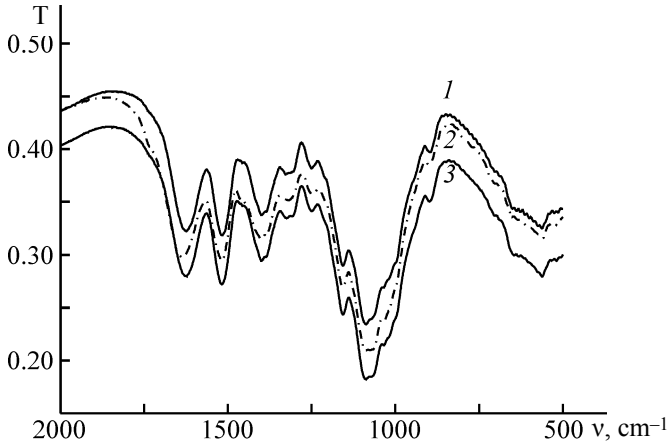

Fig. 2. IR spectra of (*1*) starting and (*2, 3*) depolymerized chitosan samples. (T) Transmission and (ν) wave number. MM: (*1*) 1.95×10^5, (2) 0.57×10^5, and (3) 0.27×10^5.

because the bands of carboxylate ions and amino groups of chitosan overlap.

All the IR spectra contain bands characteristic of chitosan. The strong bands at 1100 and 1187 cm^{-1} are associated with stretching vibrations of the carbon skeleton of macromolecules. The absorption bands at wave numbers in the ranges 1660–1610 and 1550–1485 cm^{-1} belong to asymmetric deformation vibrations of the NH_3^+ group. The band at around 1300 cm^{-1} corresponds to symmetric vibrations. The broad medium-intensity band at 1387 cm^{-1} is associated with deformation vibrations of the OH bond. The IR spectra of low-molecular destruction products hardly differ from those for the starting chitosan. It should be noted, however, that the band of amino groups at 1610 cm^{-1} is broadened in the IR spectra of the depolymerizates. This may be due to the appearance and superposition of unresolved peaks at 1730–1690 cm^{-1}, characteristic of aldehyde, carboxy, and ketone groups.

Based on 0.4% solutions of the starting chitosan and its depolymerizates, we obtained dispersions of chitosan sulfate particles by addition of a magnesium sulfate solution [12]. After the solutions were poured together, their turbidization was observed in a certain time due to the formation of particles of an insoluble product of the ionic interaction of protonated amino groups of chitosan with sulfate anions in accordance with the scheme:

$$[C_6H_9O_4\text{–}NH_3^+]_n + n/2SO_4^{2-}$$
$$\rightarrow [C_6H_9O_4\text{–}NH_3\text{---}SO_4\text{---}NH_3\text{–}C_6H_9O_4]_{n/2}\downarrow.$$

Figure 3 shows curves describing the variation with time of the optical density of the dispersions formed upon introduction of magnesium sulfate into equiconcentrated solutions optical feedback samples with various MMs in the absence of surface-active stabilizers.

Figure 3a illustrates the process in which the dispersed phase was formed for samples used to measure the optical density taken from permanently agitated dispersions. The optical density of the dispersions is determined both by the number of particles in unit volume and by the size of these particles. Therefore, the dependences in Fig. 3a cannot be used to evaluate the rate of the process represented by scheme (1). Nevertheless, it can be noted that, at the same component concentrations of the mixtures, samples with lower MM, compared with the starting chitosan, yielded dispersions wit higher optical density. This is presumably

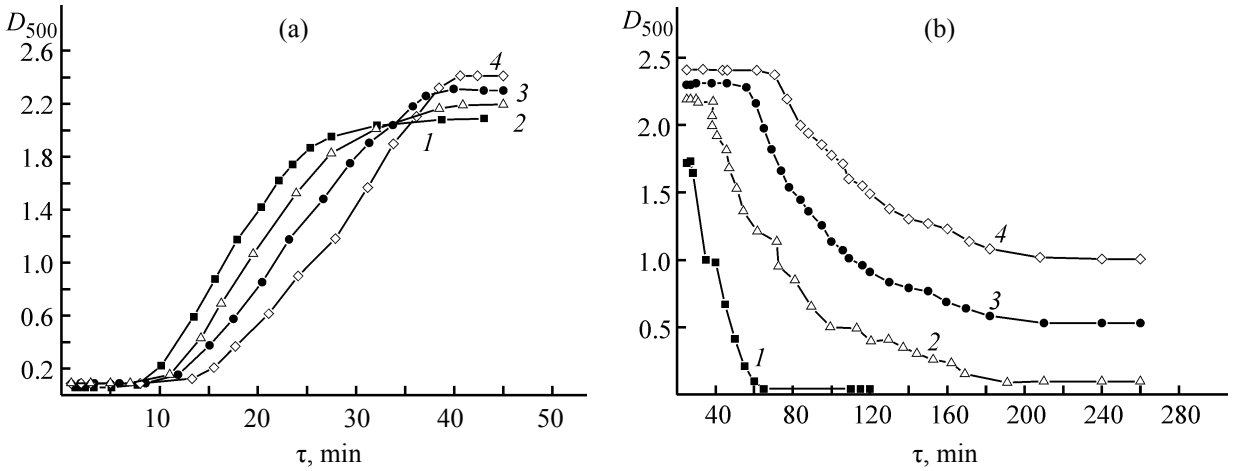

Fig. 3. Kinetic curves describing the variation of the optical density of chitosan dispersion. The curves illustrate the processes in which (a) the dispersed phase is formed under permanent agitation and (a) sedimentation occurs in the state of rest. (D_{500}) Optical density at λ = 500 nm and (τ) time. $\nu_{NH_2} : \nu_{SO_4}$ molar ratio 1 : 0.75. MM: (*1*) 1.95×10^5, (*2*) 0.93×10^5, (*3*) 56.8 kDa, and (*4*) 27.5 kDa.

due to the formation of a greater number of finer particles. In this case, an inverse correlation is observed between the MM of a sample and the limiting value reached for the optical density. For samples with smaller MMs, the slower turbidization of the solutions points to a lower aggregation rate of particles, rather than to the lower rate of their formation. It should be taken into account here that samples with small MM can form smaller particles, with these particles considerably later reaching the critical size at which they can scatter light.

It is known that particles rapidly aggregate in the absence of surface-active stabilizers [15, 17]. In the present study, no surface-active stabilizers were used, and, therefore, the upper layer of the resulting dispersions left at rest gradually clarified after a certain time due to the settling of the aggregates being formed. As follows from Fig. 3b, the sedimentation stability of the dispersions produced from samples with smaller MMs was found to exceed that of the starting chitosan. Figure 4 shows a micrograph of the dispersion obtained from chitosan with MM = 0.57×10^5 40 min after sulfate ions were introduced, in which separate particles and already formed aggregates can be seen.

To determine the size of the primary particles, we 20-fold diluted the dispersion immediately after their formation. According to published data [1], this dilution can ix the particle size because of the substantial decrease in the aggregation rate. As the MM of chitosan becomes smaller, the particle size steadily decreases (Table 1). It can also be noted that on the whole smaller widths W (nm) of the particle size distribution were obtained for destructed samples, although no correlation is observed between this quantity and the MM of chitosan. Table 1 also lists the yields of the dispersed phase for each chitosan sample. The percentage yield was calculated as the ratio between the actual mass of particles isolated from the dispersions allowed to stay for 24 h and the value calculated for the hypothetical case of 100% conversion of chitosan to an insoluble complex in accordance with scheme (1). The yield was calculated by using the averaged molecular mass of a conditional elementary unit of chitosan in the complex (MM_u), determined by the formula

$$MM_u = \frac{M(N)[100 - \omega(H_2O)]}{\omega(N)\, M(S)\, DDA}. \quad (1)$$

According to experimental data, the mass fraction of water in the product, $\omega(H_2O) = 9$ wt %; the mass fractions of nitrogen, determined by elemental analysis, are listed in Table 2. The averaged MM_u in the complex, calculated by formula (1) to be on average 217 g mol^{-1}, was little dependent on the MM of the starting chitosan samples. It follows from the data in Table 1 that the yield of the dispersed phase decreases as the MM of the starting chitosan becomes lower.

Table 1. Effect of the peroxide destruction of chitosan on the size of particles produced from this substance

Sample no.	MM × 10^5	Yield, %	d_{av}, nm	W, nm
1	1.95	95.5	1175	182
2	0.93	93.1	340	43
3	0.57	89.3	313	57
4	0.38	86.4	290	51
5	0.27	80.6	239	62
6	0.20	72.9	150	62

Table 2 presents the results of an elemental analysis of isolated and dried particles of the solid phase. The same table lists the $\nu_{SO4} : \nu_{NH2}$ ratios in the dry product, calculated from the elemental analysis data with consideration for the DDA by the formula

$$\nu_{SO_4} : \nu_{NH_2} = \frac{\omega(S)M(N)}{\omega(N)M(S)DDA}. \quad (2)$$

It follows from the data in Table 2 that changes in the MM of chitosan affect the composition of the isolated dry product only slightly. The molar ratio between the

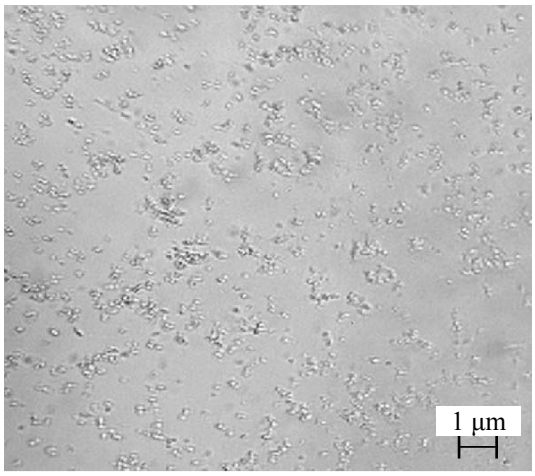

Fig. 4. Micrograph of a dispersion produced from chitosan with MM = 0.57×10^5 in 40 min after the introduction of sulfate ions.

Table 2. Results of an elemental analysis of the insoluble chitosan sulfate complex

Sample no.	MM × 10^5	$\nu_{SO_4} : \nu_{NH_2}$	ω, %			
			N	C	H	S
1	1.95	0.45	5.96	30.60	5.79	5.09
2	0.93	0.46	5.82	30.71	6.31	5.02
3	0.57	0.46	5.84	30.87	6.45	5.02
4	0.38	0.46	5.75	30.94	6.03	4.99
5	0.27	0.45	5.75	30.98	6.81	4.89
6	0.20	0.46	5.75	31.07	6.09	4.92

components in the particles changes insignificantly, within the range 0.45–0.46, without reaching the calculated value of 0.5 corresponding to the 100% binding of all amino groups. A similar result was obtained in [12] for a wide range of starting mixture compositions.

Figure 5 shows how the pH of the medium affects the magnitude and sign of the ζ-potential of chitosan sulfate particles produced from the starting chitosan (MM = 1.95 × 10^5) and its depolymerizates with MM of 0.57 × 10^5 and 0.27 × 10^5. It can be seen that the runs of the curves for the depolymerized samples and the starting chitosan are strongly different. This is manifested in a decrease in the positive values of the ζ-potential in the acid range of pH values and in an increase in the negative values of this parameter at pH > 5. The isoelectric point is observed for depolymerized samples at pH 5.0. For the starting chitosan, a slight departure of the curve into the negative region is observed at pH 8. It should be noted that negative values of the ζ-potential were obtained for the first time. As a rule, the literature gives positive values of the ζ-potential for chitosan sulfate particles in a wide range of pH values [17, 18]. An explanation provide by some authors is that not all amino groups of chitosan in the particles being formed are bound with sulfate ions, and just the remaining free groups are responsible for the positive charge of the particles [3]. With increasing pH, the degree of protonation of free amino groups decreases. At pH > 6.2, amino groups of chitosan must be deprotonated (pK_a 6.2–6.3). At higher pH values, the negative charge of particles based on chitosan samples with lowered MM is presumably due to the dissociation of carboxy groups formed in the course of the preceding oxidative destruction. Despite the comparatively close MM values of the depolymerizates tested in the given experiment, it should be taken into account that the samples with MM 0.57 × 10^5 and 0.27 × 10^5 were obtained at peroxide destruction durations of 60 and 120 min, respectively. A longer (by a factor of 2) exposure to the oxidizing agent and thermal treatment determined the formation of a larger amount of oxygen-containing groups in chitosan, which was manifested in a changed pH dependence of the ζ-potential of chitosan sulfate particles.

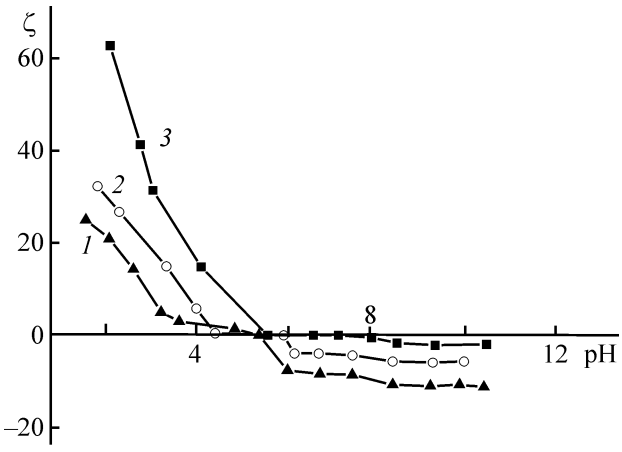

Fig. 5. Dependence of the ζ-potential of chitosan sulfate particles on the pH of the medium. MM: (*1*) 0.27 × 10^5, (*2*) 0.57 × 10^5, and (*3*) 1.95 × 10^5.

CONCLUSIONS

(1) The effect of the oxidative destruction of chitosan by hydrogen peroxide on the processes of formation and sedimentation of dispersed-phase particle in its dilute solutions in the presence of sulfate ions was studied.

(2) It was found that the size of chitosan sulfate particles steadily decreases as the MM of chitosan becomes smaller. No correlation was found between the width of the particle size distribution and the MM of chitosan.

(3) It was shown that the $\nu_{SO_4} : \nu_{NH_2}$ molar ratio in chitosan sulfate particles is independent of the MM of chitosan and varies within the range 0.45–0.46.

(4) A pH dependence of the sign of the ζ-potential with an isoelectric point at pH 5.0 was observed for particles based on destructed chitosan.

REFERENCES

1. Mayyas, M.A. and Al-Remawi, M.M.A., *Am. J. Appl. Sci.,* 2012, vol. 9, no. 7, pp. 1091–1100.
2. Loh Jing, W., Schneider, J., Carter, M.M., et al., *J. Pharm. Sci*., 2010, vol. 99, no. 10, pp. 4326–4336.
3. Berthold, A, Cremer, R., and Kreuter, J., *J. Controlled Release*, 1996, vol. 39, pp. 19–25.
4. Janes, K.A. and Alonso, M.J., *J. Appl. Polym. Sci*., 2003, vol. 88, no. 12, pp. 2769–2776.
5. Fernandes, A.L.P., Morais, W.A., and Santos, A.I.B., *Colloid Polym. Sci*., 2005, vol. 284, no. 1, pp. 1–9.
6. Qandil, A.M., Obaidat, A.A., Ali, M.A.M., et al., *J. Solution Chem*., 2009, vol. 38, pp. 695–712.
7. Il'ina, A.V., Tkacheva, Yu.V., and Varlamov, V.P., *J. Appl. Biochem. Microbiol*., 2002, vol. 38, no. 2, pp. 112–115.
8. Muzzarelli, R.A.A., Tanfani, F., and Emanuelli, M., *J. Membr. Sci.,* 1983, vol. 16, pp. 295–308.
9. Mullagariev, I.R., Monakov, Yu.B., and Galiaskarova, G.G., *Dokl. Chem. Technol*., 1995, vol. 345, no. 2, pp. 179–184.
10. Nud'ga, L.A., Plisko, E.A., and Danilov, S.N., *Russ. J. Gen. Chem*., 1973, vol. 43, no. 12, pp. 2736–2749.
11. Wang, W., Bo, S., Li, S., and Qin, W., *Int. J. Biol. Macromol*., 1991, vol. 13, pp. 381–387.
12. Mezina, E.A. and Lipatova, I.M., *Russ. J. Appl. Chem*., 2014, vol. 87, no. 6, pp. 820–824.
13. Shao, J., Yang, Y, and Zhong, Q., *Polym. Degrad. Stab*., 2003, vol. 82, no. 3, pp. 395–398.
14. Fedoseeva, E.N., Smirnova, E.N., Sorokina, M.A., and Pastukhov, M.O., *Russ. J. Appl. Chem*., 2006, vol. 79, no. 5, pp. 845–849.
15. Qin, C, Du, Y, Xiao, L., et al., *J. Appl. Polym. Sci*., 2002, vol. 86, no. 7, pp. 1724–1730.
16. Kassai, M.R., *J. Agric. Food Chem*., 2009, vol. 57, pp. 1667–1676.
17. Trindade Neto, C.G, Fernandes, A.L.P., Santos, A.I.B., Morais, W.A., et al., *Polym. Int*., 2005, vol. 54, no. 4, pp. 659–666.
18. Tavaresa, I.S., Caronib, A.L.P.F., Dantas Netob, A.A., et al., *Colloids Surf., B*, 2012, vol. 90, pp. 254–258.